Appl. Phys. B 45, 237–243 (1988)

Applied Physics B Photophysics and Laser Chemistry

Nonlinear Optical Properties of Organic Dye Dimer-Monomer Systems

S. Speiser*, V. H. Houlding, and J. T. Yardley

Allied-Signal Inc., Engineered Materials Sector, P.O. Box 1087R, Morristown, NJ 07960, USA

Received 9 November 1987/Accepted 16 January 1988

Abstract. An analysis is provided for the discussion of nonlinear optical properties of aggregated dye systems. The intensity-dependent transmission of fluorescein solutions excited by nanosecond dye laser pulses is shown to fit a monomer-dimer equilibrium shifted towards monomer formation by excitation. The implications for spatial light modulation and other nonlinear optical applications are discussed.

PACS: 33, 42.65, 42.70

Optical switches, optical bistable devices and spatial light modulators (SLMs) are important key elements in optical computers and in optical data processing systems [1]. In recent years this field has advanced tremendously; however, the lack of appropriate materials to implement theoretical design of optical hardware has been considered as a bottleneck in realizing the potential of the field [2]. Organic materials may provide ideal media needed for this optical hardware [3]. It is already known that such materials exhibit the high nonlinear optical susceptibilities which are necessary for optical data processing. Thus far, most experiments on organic nonlinear optical materials have concentrated on second-harmonic generation (SHG) [3, 4]; however, in recent years optical modulation [5], optical bistability [6], optical phase conjugation [7] and related phenomena have been studied in these systems.

An all-optical device based on appropriate organic materials will operate on the intensity-induced changes in the complex index of refraction, i.e., the absorptive and dispersive properties of the medium due to intensity-induced population changes. Due to their highly allowed electronic transitions, organic dyes have long been used in many electrooptical applications such as Q-switching [8], modelocking [8] and as an active laser medium [9]. More recently their nonlinear optical properties have been utilized in four-wave mixing experiments [10], optical phase conjugation [12, 13] real-time holography [11, 12] and in optical-bistability experiments [13–15].

Polymer films doped with dye molecules have been considered as an appropriate medium for device fabrication. In many cases dimer and higher aggregated forms of the dyes have been overlooked [7, 11], although as we will show in this paper, the aggregation state can have a marked effect on the nonlinear optical properties of the system. More recently it has been demonstrated that an aggregated dye-polymer thin film can exhibit high efficiency of second harmonic generation [16]. It is the purpose of this paper to provide a general analysis of the laser-induced optical nonlinearities in such systems and to discuss several applications of this unique behavior.

Intensity Dependent Complex Index of Refraction for a Dimer-Monomer System

In this section we discuss interaction of light with a nonlinear medium consisting of an ensemble of large aggregated organic molecules. The rich variety of excitation routes in these molecules gives rise to a number of different intensity dependences of the complex nonlinear index of refraction. Figure 1 depicts a dimer-monomer molecular system together with relevant rate parameters. The monomer-dimer equilib-

* On sabbatical leave. To whom correspondence should be addressed at: Department of Chemistry, Technion-Israel Institute of Technology, Haifa 32000, Israel

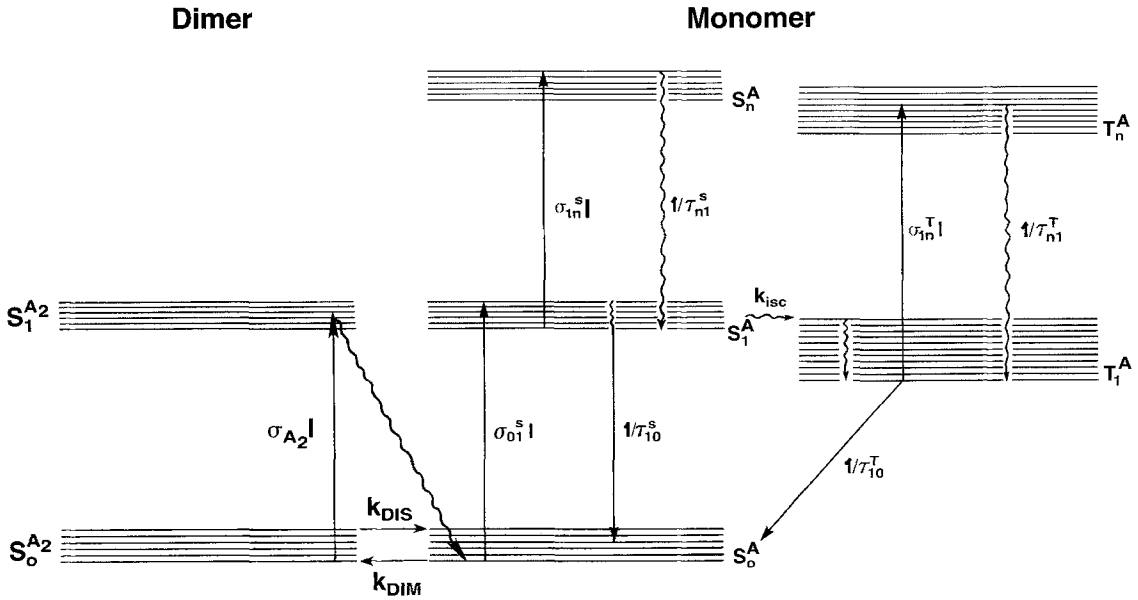

Fig. 1. Schematic level diagram for a dimer(A)-monomer(A_2)/dye system, triplet (T_i) manifolds, radiative (→) and nonradiative (⇝) transitions. Absorption cross-sections are σ_{ij}, τ_{ji} are the level lifetime and k_{ISC} denotes the intersystem crossing rate. Dissociation of the dimer at its S_1 state is fast compared to the excitation process

rium of the dye system is shifted towards the monomer form under laser excitation, the kinetics of which can be described by

$$A_2(S_0) \underset{k_{DIM}}{\overset{k_{DIS}}{\rightleftarrows}} 2A(S_0), \tag{1}$$

$$A_2(S_0) \xrightarrow{\sigma_{A_2} I} 2A(S_0), \tag{2}$$

where k_{DIS} and k_{DIM} are dimer dissociation and association rate constants, respectively, and σ_{A_2} is the absorption cross section of the dimer excited by laser of intensity I. Step (2) involves excitation of dimers to their first excited singlet state followed by rapid dissociation to monomers. Even for nanosecond excitation, steady state conditions are reached [17] for most dyes. Under these conditions we obtain that:

$$K(I) = [A_2]/[A]^2 = k_{DIM}/(k_{DIS} + \sigma_{A_2} I) = K/[1 + \sigma_{A_2} I/k_{DIS})], \tag{3}$$

where

$$K = k_{DIM}/k_{DIS} \tag{4}$$

is the association equilibrium constant.

The monomer behaves as a molecular absorber where both singlet S and triplet T electronic state manifolds are involved. The dynamics of this system can be described using the rate equation approximation.

$$d\mathbf{N}/dt = \hat{\mathbf{O}}\mathbf{N}, \tag{5}$$

where $\mathbf{N}$ is the monomer population vector given by transposed form

$$\tilde{\mathbf{N}} = (N^A(S_0), N^A(S_1), N^A(S_n), N^A(T_1), N^A(T_n)). \tag{6}$$

At steady state, the total monomer concentration N is given by

$$N = N^A = [N^{A_2}/K(I)]^{1/2}. \tag{7}$$

The rate constants operator, $\hat{\mathbf{O}}$, for the case of a vibrationally relaxed S_1^A, is given by

$$\hat{\mathbf{O}} = \begin{pmatrix} -\sigma_{01}^S I & 1/\tau_{10}^S & 0 & 1/\tau_{10}^T & 0 \\ \sigma_{01}^S I & -(1/\tau_{10}^S + k_{ISC} + \sigma_{1n}^S I) & 1/\tau_{n1}^S & 0 & 0 \\ 0 & \sigma_{1n}^S I & -1/\tau_{n1}^S & 0 & 0 \\ 0 & k_{ISC} & 0 & -\sigma_{1n}^T I + 1/\tau_{10}^T & 1/\tau_{n1}^T \\ 0 & 0 & 0 & \sigma_{1n}^T I & -1/\tau_{n1}^T \end{pmatrix} \tag{8}$$

with $\tau_{ij}^{S,T}$: decay time of the i level to the j level in the S or T manifolds, respectively, k_{ISC}: intersystem crossing rate constant, $\sigma_{ij}^{S,T}$: absorption cross section for the $i \rightarrow j$ transition in the S or T manifolds, respectively, and I: local pump light intensity.

All states excited higher than the lower excited state are denoted by n; the ground state is S_0^A.

For cw or even for nanosecond pulse excitation a steady-state solution, $d\mathbf{N}/dt=0$ of (5) is sufficient, yielding the intensity dependent populations

$$\mathbf{N}(I)=[N(S_0^A)/(k_{ISC}+1/\tau_{10}^S)]\begin{pmatrix} k_{ISC}+1/\tau_{10}^S \\ \sigma_{01}^S I \\ \sigma_{01}^S\sigma_{1n}^S\tau_{n1}^S I^2 \\ \sigma_{01}^S k_{ISC}\tau_{10}^T I \\ \sigma_{01}^S k_{ISC}\tau_{10}^T\sigma_{1n}^T\tau_{n1}^T I^2 \end{pmatrix}, \tag{9}$$

where the population of S_0^A is given by

$$N(S_0^A)=N/[1+\sigma_{01}^S\tau_{10}^S(1+k_{ISC}\tau_{10}^T)I/(1+k_{ISC}\tau_{10}^S) + \sigma_{01}^S\tau_{10}^S(\sigma_{1n}^S\tau_{n1}^S + k_{ISC}\tau_{10}^T\sigma_{1n}^T\tau_{n1})I^2/(1+k_{ISC}\tau_{10}^S)] \tag{10}$$

and N is the total monomer molecular concentration, given by (7).

The origin of the optical nonlinearity in these molecules is the intensity-dependent population. Each level is characterized by an absorption cross-section and by an index of refraction which are functions of the excitation wavelength, i.e. their specific electronic spectra. The change in these parameters between different levels is due mainly to contribution of specific resonances from the particular level. The contribution for the nonlinear complex index of refraction from the monomer can be written as the scalar product

$$\eta(I)=\mathbf{N}(I)\cdot\boldsymbol{\eta}'+\mathrm{i}(\lambda_0/4\pi)\mathbf{N}(I)\cdot\boldsymbol{\sigma}=\eta^D(I)+\mathrm{i}(\lambda_0/4\pi)\alpha(I), \tag{11}$$

where α is the monomer contribution to the absorption coefficient. Its contribution to the real part of the refractive index (dispersive contribution) $\boldsymbol{\eta}'=\boldsymbol{\eta}^D/N$ is given by

$$\boldsymbol{\eta}'=(\eta'_{S_0},\eta'_{S_1},\eta'_{S_n},\eta'_{T_1},\eta'_{T_n}). \tag{12}$$

The absorption cross sections [absorptive contribution to $\eta(I)$] are given by

$$\boldsymbol{\sigma}=(\sigma_{01}^S,\sigma_{1n}^S,0,\sigma_{1n}^T,0), \tag{13}$$

assuming negligible absorption for levels $n>1$.

Using (9 and 13) the absorption coefficient can be obtained

$$\alpha(I)=\mathbf{N}(I)\cdot\boldsymbol{\sigma}+[C-N(I)/2]\sigma_{A_2} =\alpha_0(1+BI)/(1+\gamma I+\delta I^2)+(C-N/2)\sigma_{A_2}, \tag{14}$$

where the various coefficients in (14) are defined in Table 1 for various excitation routes and C is the total concentration of dye species.

The real part of the refractive index is obtained as a weighted sum of the indices of S_0^A, S_1^A, and T_1^A assuming that S_n^A and T_n^A are not significantly populated. Thus the real part of $\eta(I)$ is

$$\eta^D=(A'+B'I)/(1+\gamma I+\delta I^2)+\gamma', \tag{15}$$

where A', B', and γ' are given in Table 1 for various excitation routes. Equations (14, 15) form a basis for calculating various nonlinear optical properties of an aggregated dye system. They require detailed information about the various molecular parameters. There are, however, situations where the discussion can be simplified considerably. For example, at pump intensities that are too low to induce any photoquenching of the monomer fluorescence due to excitation of $A(S_1)$ to higher singlet states, the intensity dependent absorption coefficient becomes

$$\alpha(I)=\{[8K(I)C+1]^{1/2}+1\}(\sigma_{01}^S - \sigma_{A_2}/2)/4K(I)+C\sigma_{A_2}/2. \tag{16}$$

Table 1. Definition of rate parameters utilized in obtaining the intensity dependent complex of index of refraction $\eta(I)$ for the various excitation routes depicted in Fig. 1

	Excitation route			
Parameter	Full scheme S_n ↑ $S_0\rightarrow S_1\rightsquigarrow T_1\rightarrow T_n$	Route I $S_0\rightarrow S_1\rightsquigarrow T_1$	Route II $S_0\rightarrow S_1\rightsquigarrow T_1\rightarrow T_n$	Route III[a] $S_0\rightarrow S_1\rightsquigarrow T_1\rightarrow T_n^*$
α_0	$N\sigma_{01}^S$	$N\sigma_{01}^S$	$N\sigma_{01}^S$	$N\sigma_{01}^S$
B[b]	$(\sigma_{1n}^S+k_{ISC}\tau_{10}^T\sigma_{1n}^T)/k_1=\sigma_{1n}^S/k_1+B_1$	0	B_1	B_1
γ	$\sigma_{01}^S\tau_{10}^S(1+k_{ISC}\tau_{10}^T)/k_1=C_1$	γ_1	γ_1	γ_1
δ	$\sigma_{01}^S\tau_{10}^S(\sigma_{1n}^S\tau_{n1}^S+k_{ISC}\tau_{10}^T\sigma_{1n}^T\tau_{n1}^T)/k_1=\delta_1+\delta_2$	0	δ_2	δ_2
A'	$N\eta'_{S_0}=\eta_{S_0}$	$N\eta'_{S_0}=\eta_{S_0}$	$N\eta'_{S_0}=\eta_{S_0}$	Not discussed
B'	$N\sigma_{01}^S\tau_{10}^S[\eta_{S_1}+\eta_{T_1}k_{ISC}\tau_{10}^S]/k_1=B'_1+B'_2$	B'_2	B'_2	Not discussed
γ'	$(C-N/2)\eta'_{A_2}$	γ'	γ'	Not discussed

[a] T_n^* denotes population trapping at T_n via a particular mechanism, or a photochromism isomerization

[b] $k_1=1+k_{ISC}\tau_{10}^S$

At low intensities α approaches

$$\alpha(I)=(\sigma^S_{01}-\sigma_{A_2}/2)\,[(1+8KC)^{1/2}+1]\,(1+\sigma_{A_2}I/k_{DIS})/4K+C\sigma_{A_2}/2. \quad (17)$$

This enhanced absorption should be manifested in basically two-photon induced fluorescence of monomers photoquenched at higher light intensities. Following standard photoquenching analysis [17], we find that the fluorescence intensity Y is given by

$$Y=\phi\sigma_{A_2}\sigma^S_{01}I^2\tau_p/(1+\tau^S_{10}\sigma^S_{01}I+\tau^S_{10}\sigma^S_{01}\tau^S_{n1}\sigma^S_{1n}I^2), \quad (18)$$

where ϕ is the fluorescence quantum yield and τ_p is the laser pulse width.

Experimental

A Nd-YAG laser harmonic generated light (Quanta Ray DCR3) was used to excite a dye laser (Quanta Ray PDL-2). Dye laser light was used to excite the fluorescein solutions. Laser intensities (at 480 nm) were monitored by Hamamatsu 1188-06 PIN photodiodes and analyzed by a Tektronix 2430 digital oscilloscope interfaced to an IBM XT computer. Pump and probe experiments (at 480 nm) were performed using a 1% split off beam of the exciting laser, probing at a right angle to the input beam. Laser induced fluorescence data (at 520 nm) were obtained by using a PTR monochromator and a Hamamatsu R928 photomultiplier. Spectrophotometric measurements were carried out on a Perkin-Elmer 330 spectrophotometer.

Fluorescein (Kodak laser grade) was used without further purification. Solutions in absolute ethanol were used within 24 h of preparation. Thin films of fluorescein in PMMA were prepared by a standard spin coating technique.

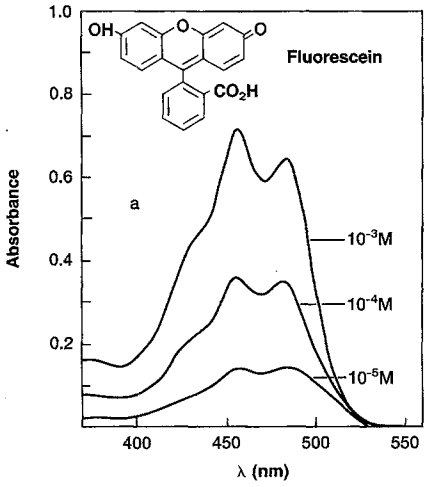

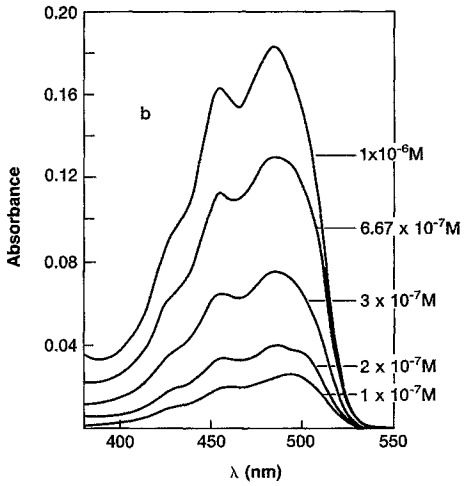

Fig. 2a, b. Absorption spectra for fluorescein solutions in ethanol (1 cm path length) (a) high concentration spectra (b) low concentration data

Results

Figure 2 shows the absorption spectrum of fluorescein in ethanol at various concentrations. It is clear that Beer's law is not obeyed, mainly because of dimer formation [18–20]. Similar spectra were obtained for fluorescein PMMA thin films. The dimer(A_2)-monomer(A) equilibrium is described by (1). The effective absorption coefficient of the dye system is given by

$$\beta=\varepsilon_A(C-2X)+\varepsilon_{A_2}X, \quad (19)$$

where X is the equilibrium molar concentration of dimers and ε_A and ε_{A_2} are the molar excitation coefficients of the monomer and dimer species, respectively. From a simple equilibrium stoichiometry we

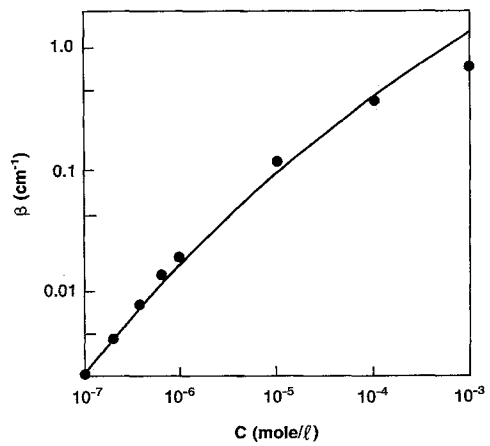

Fig. 3. Absorption coefficient β (at 480 nm) *vs* concentration for fluorescein, the solid line is the best fit curve to (20)

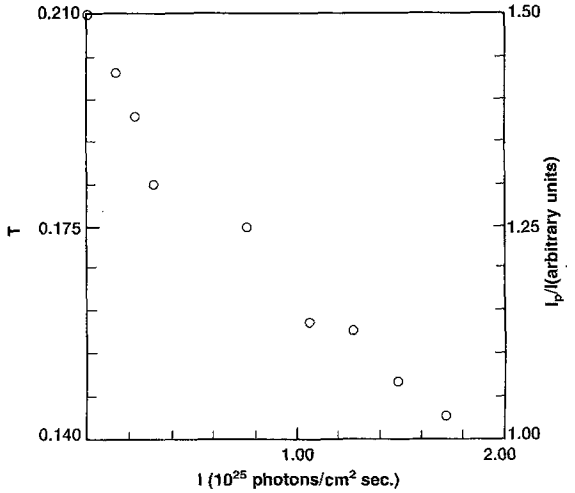

Fig. 4. Intensity modulation of the probe beam by the pumping laser, at 480 nm

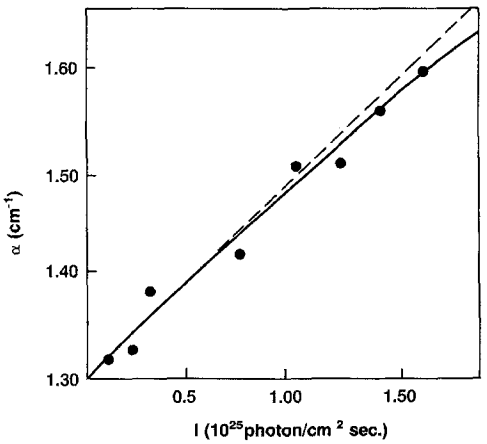

Fig. 5. Intensity dependent absorption coefficient, α for fluorescein 10^{-3} mole/l ethanol solution at 480 nm. The solid line is the best fit curve to (16), the dashed line is the linear fit to (17)

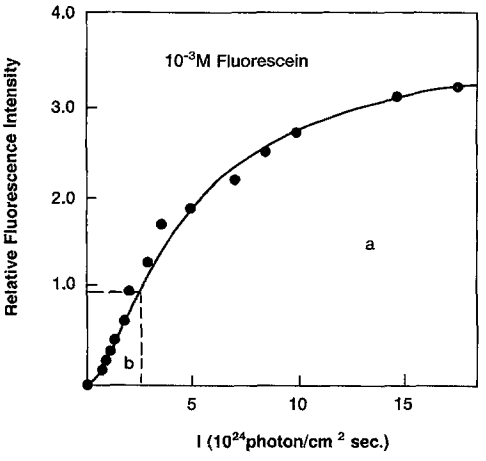

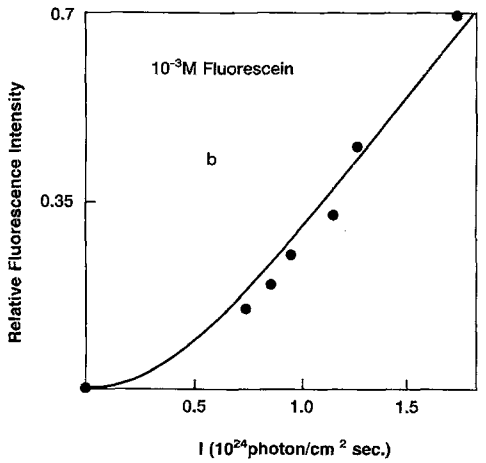

Fig. 6. (a) Laser induced fluorescence (520 nm emission) intensity for 10^{-3} mole/l fluorescein/ethanol solution (480 nm excitation). (b) A blow up of the $0\text{–}2 \times 10^{24}$ photon/cm^2 s region showing the quadratic dependence of the concencutive two-photon induced fluorescence resulting from dimer photolysis followed by monomer absorption. The solid line is the best fit to (18)

obtain that

$$\beta = [(8KC+1)^{1/2}+1](\varepsilon_A - \varepsilon_{A_2}/2)/4K + C\varepsilon_{A_2}/2, \quad (20)$$

where $\beta = \alpha/2.3$.

At extremely low concentrations, Beer's law behavior is approached yielding $\varepsilon_A = 2 \times 10^4$ l/mole cm. Equation (20) can be fitted to the β vs. C data of Fig. 2. The best fit curve is shown in Fig. 3 yielding $K = 10^5$ l/mole and $\varepsilon_{A_2} = 260$ l/mole cm at 480 nm. The deviation at high concentration is probably due to the presence of higher aggregates.

Figure 4 shows the results of the 480 nm laser pump and probe experiments for 10^{-3} mole/l fluorescein in ethanol. The probe intensity I_p is modulated by the pump intensity I due to the transient formation of highly absorbing monomer. The corresponding intensity dependent absorption coefficient is shown in Fig. 5 where a good fit is made with (16) and (17).

A more sensitive method of determining the aggregation state of the dye is provided by the laser induced fluorescence studies. Figure 6 shows a least square fit of (18) to laser induced fluorescence data for 10^{-3} mole/l fluorescein solutions. The value obtained from the best fit for $\tau_{10}^S \sigma_{01}^S$ is in good agreement with the calculated one. We may thus conclude that at these concentrations the fluorescein system is characterized by an absorption coefficient which is an increasing function of incident laser intensity. At 10^{-6} mole/l, fluorescein is mostly in the monomer form and laser induced fluorescence studies are typical of photoquenching process [17] for which

$$Y = \phi \sigma_{01}^S I/(1 + \tau_{10}^S \sigma_{01}^S I + \tau_{10}^S \tau_{n1}^S \sigma_{01}^S \sigma_{1n}^S I^2). \quad (21)$$

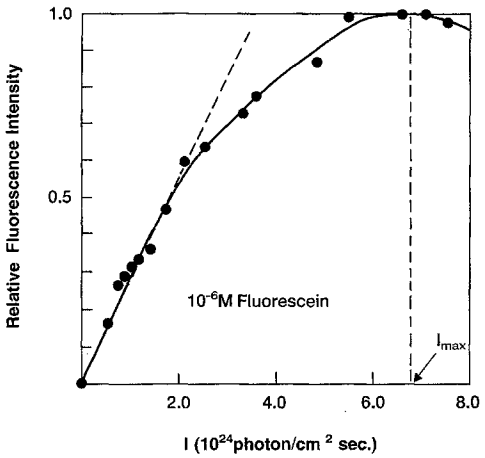

Fig. 7. Intensity dependence of laser induced fluorescence (520 nm emission) of 10^{-6} mole/l fluorescein (480 nm excitation)

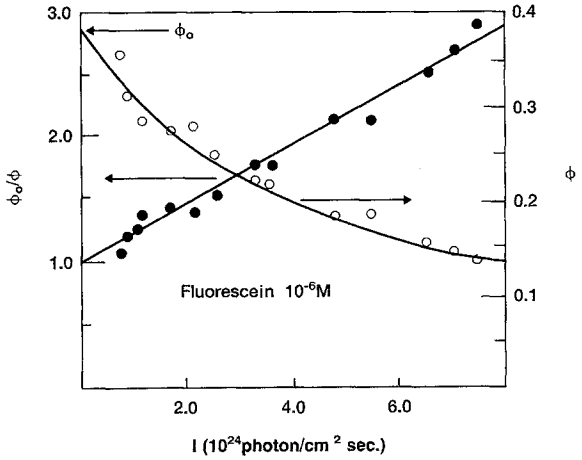

Fig. 8. Photoquenching plots [17] for 10^{-6} mole/l fluorescein

This behavior is exemplified in Fig. 7 for fluorescein monomers. The maximum Y occurs at [17],

$$I_{\max}=(\tau_{10}^S\sigma_{01}^S\tau_{n1}^S\sigma_{1n}^S)^{-1/2}. \tag{22}$$

The reciprocal relative quantum yield is given by [17],

$$\phi_0/\phi=1+\tau_{10}^S\sigma_{1n}^S I, \tag{23}$$

where ϕ_0 is the limit of ϕ for $I\to 0$.

Figure 8 shows the fit of the experimental relative quantum yield to (23). For $\tau_{10}=3.9$ ns [21] we obtain that $\sigma_{1n}^S=5\times10^{-17}$ cm^2/molec, and $\tau_{n1}^S=2\times10^{-10}$ s.

Aggregation can be also manifested in modification of the fluorescence spectrum and quantum yield. This was recently demonstrated by Penzkoffer and Leupacher [22] for rhodamine 6G solutions. While spectroscopy can give some information about the structure of the dye dimers, it does not yield any photophysical data. Thus intensity dependent laser induced fluorescence data of the kind demonstrated here can complement the spectroscopic and quantum yield measurement.

Discussion

We have demonstrated that the spectral properties of fluorescein in ethanol solution are well described in terms of a dimer-monomer equilibrium which favors dimer formation at concentrations higher than 10^{-4} mole/l. A combination of spectrophotometry, intensity dependent laser induced fluorescence and laser pump and probe studies indicate that this equilibrium is shifted towards monomer formation at high pump intensities. The efficiency of this process can be evaluated in terms of $\partial\alpha(I)/\partial I$. From (17) we obtain that

$$\partial\alpha(I)/\partial I=(\sigma_{01}^S-\sigma_{A_2})[1+(1+8KC)^{1/2}]\sigma_{A_2}/4k_{DIS}K. \tag{24}$$

For most practical systems $\sigma_{01}^S\gg\sigma_{A_2}$ and $KC\gg1$ so that (24) reads

$$\partial\alpha/\partial I=[\sigma_{01}^S\sigma_{A_2}(2C/K)^{1/2}]/2k_{DIS}$$
$$=\sigma_{01}^S\sigma_{A_2}(2KC)^{1/2}/2k_{DIM}. \tag{25}$$

From the slope of Fig. 5 we obtain $\partial\alpha/\partial I=2\times10^{-26}$ cm s/photon, which together with our measured values for K, σ_{01}^S, and σ_{A_2} yields $k_{DIM}=2.7\times10^{-8}$ cm^3/s$=1.6\times10^{13}$ l/mole s. This high value for k_{DIM} is indicative of high recombination rate for fluorescein monomers typical of recombination processes inside a solvent cage [23]. The corresponding dissociation rate constant is $k_{DIS}=1.6\times10^8$ s^{-1}. Table 2 summarizes the molecular parameters obtained for fluorescein using our kinetic analysis. Spectrophotometric data show that the same dimerization equilibrium exists in fluorescein doped PMMA samples.

The large difference between σ_{01}^S and σ_{A_2} results in a highly nonlinear optical absorption for this system. It is manifested in nonlinear laser induced fluorescence,

Table 2. Molecular parameters for the fluorescein dimer-monomer system in ethanol solution for 480 nm excitation

Parameter	Value
K	1.67×10^{-16} cm^3/molec
k_{DIM}	2.7×10^{-8} cm^3/s
k_{DIS}	1.6×10^8 s^{-1}
σ_{A_2}	10^{-18} cm^2/molec
σ_{01}^S	7.6×10^{-17} cm^2/molec
σ_{1n}^S	5×10^{-17} cm^2/molec
τ_{10}^S	3.9 ns [21]
τ_{n1}^S	0.2 ns

in the intensity modulation of the 480 nm probe beam and in a recent observation of optical bistability for this system in ethanol solution and in thin doped polymer film [15]. From (25) one can estimate the practical upper limit for a dimer-monomer system. For $\sigma_{01}^{S}=4\times10^{-16}$ cm^2/molec, $\sigma_{A_2}=10^{-17}$ cm^2/molec, $K=10^{-14}$ cm^3/molec, at 6×10^{17} molec/cm^3 (10^{-3} mole/l) concentration, we obtain for a recombination rate constant of 3×10^{-8} cm^3/s, that $\partial\alpha/\partial I=2.5\times10^{-25}$ cm s/photon, or about 0.6 cm^{-1}/(MW/cm^2). We may thus conclude that dimer-monomer systems offer a number of advantages for some nonlinear optical applications due to the relatively large dimer-monomer absorption cross section difference and the rapid response time due to in-cage recombination process. In addition, these systems are photochemically stable since dimerization involves the photochemically active sites of the monomer unit. The rather high $\partial\alpha/\partial I$ value may be utilized in optical limiters applications, or as a spatial light modulator with faster response time than that offered by more traditional photochromic systems [5]. The recently observed optical bistability in fluorescein [15] indicates another potential application of dimer-monomer dye systems. One, of course, should be aware of complications due to thermal energy dissipation at the relatively high pumping rates required for achieving the nonlinear optical response. However, in cases where the monomer absorbs mainly in its triplet manifold, a high $\partial\alpha/\partial I$ may be obtained at much lower pump intensities but with a much slower response time.

Since fluorescein and similar dyes are being used for various types of nonlinear optical applications, the complications as well as the advantages of the inherent dimer-monomer nature of the system should be taken into account. It may well be that some of the recent studies of nonlinear optical response of fluorescein involved dimerized systems which were overlooked in interpreting experimental results [11].

In conclusion, we note that the present paper provides us with a general analysis of the nonlinear optical properties of dimer-monomer dye systems and a consistent set of specific parameters for fluorescein solutions. While fluorescein may not be the ideal case for such a system, its evaluation may lead to construction of more efficient dimer-monomer optically nonlinear systems.

Acknowledgement. We are grateful to Mr. F. L. Chisena for his help in some of the measurements.

References

1. F.T.S. Yu: *Optical Information Processing* (Wiley, New York 1983)
2. A.R. Tanguay, Jr.: Opt. Eng. **24**, 2 (1985)
3. D.S. Chemla, J. Zyss: *Nonlinear Optical Properties of Organic Molecules and Crystals* (Academic, New York 1987)
4. D.J. Williams (ed.): *Nonlinear Optical Properties of Organic and Polymeric Materials*, ACS Symp. Series 233 (ASC, Washington, DC 1983)
5. C.J.G. Kirkby, I. Bennion: IEE Proc. **133**, 98 (1986)
6. M. Orenstein, J. Katriel, S. Speiser: In *Methods of Laser Spectroscopy*, ed. by Y. Prior, A. Ben-Reuven, M. Rusenbluh (Plenum, New York 1986), pp. 335–339. Proc. SPIE **700**, 96 (1986); Phys. Rev. A **35**, 2157 (1987)
7. M.A. Kramer, W.R. Tompkin, R.W. Boyd: Phys. Rev. A **34**, 2026 (1986)
8. A. Yariv: *Quantum Electronics* (Wiley, New York 1975)
9. F.P. Schafer (ed.): *Dye Lasers*, Topics Appl. Phys. **1** (Springer, Berlin, Heidelberg 1969)
10. H. Fujiwara, K. Nakagawa: J. Opt. Soc. Am. B **4**, 121 (1987)
11. T. Todorow, L. Nikolova, N. Tumova, V. Dragostinova: Opt. Quant. Electron. **13**, 209 (1981); IEEE J. QE-**32**, 1262 (1986)
12. Y. Silberberg, I. Bar-Joseph: Opt. Commun. **39**, 265 (1981); **41**, 455 (1982)
13. Z.F. Zhu, E.M. Garmire: IEEE J. QE-**19**, 1495 (1983)
14. M.C. Rushford, H.M. Gibbs, J.L. Jewell, N. Peyghambarian, D.A. Weinberger, C.F. Li: In *Optical Bistability* 2, ed. by C.M. Bowden, S.L. McCall (Plenum, New York 1983) pp. 345–352
15. S. Speiser, F.L. Chisena: SPIE **824** (1987) (in press)
16. J. Wang: Chem. Phys. Lett. **126**, 209 (1986)
J. Wang, M. Berenstein, S.H. Stevenson: SPIE **682**, 50 (1986)
17. S. Speiser, N. Shakkour: Appl. Phys. B **38**, 191 (1985)
18. R.W. Chambers, T. Kajiwara, D.R. Kearns: J. Phys. Chem. **78**, 380 (1974)
19. I. Lopez Arbeloa: J. Chem. Soc., Faraday Trans., 2. **77**, 1725 and 1735 (1981)
20. W.E. Ford: J. Photochem. **37**, 189 (1987)
21. G. Porter, E.S. Reid, C.J. Tredwell: Chem. Phys. Lett. **29**, 469 (1974)
22. A. Penzkoffer, W. Leupacher: J. Lumin. **37**, 61 (1987)
23. K.B. Eisenthal: Ann. Rev. Phys. Chem. **28**, 207 (1977); in *Ultrashort Light Pulses*, ed. by S.L. Shapiro, Topics Appl. Phys. **18** (Springer, Berlin, Heidelberg 1977) Chap. 6